Cancer Letters 460 (2019) 29–40

Contents lists available at ScienceDirect

Cancer Letters

journal homepage: www.elsevier.com/locate/canlet

Original Articles

Sublethal heat treatment of hepatocellular carcinoma promotes intrahepatic metastasis and stemness in a VEGFR1-dependent manner

Li Tan[a,1], Shuling Chen[b,1], Guangyan Wei[a,1], Yue Li[c], Junbin Liao[a], Huilin Jin[a], Ying Zou[d], Manling Huang[e], Zhenwei Peng[f], Yu Guo[g], Sui Peng[h,e,c], Lixia Xu[d,c,**], Ming Kuang[a,b,c,*]

[a] Department of Liver Surgery, First Affiliated Hospital, Sun Yat-sen University, Guangzhou, 510080, China
[b] Division of Interventional Ultrasound, First Affiliated Hospital, Sun Yat-sen University, Guangzhou, 510080, China
[c] Precision Medicine Institute, First Affiliated Hospital, Sun Yat-sen University, Guangzhou, 510080, China
[d] Department of Oncology, First Affiliated Hospital, Sun Yat-sen University, Guangzhou, 510080, China
[e] Department of Gastroenterology, First Affiliated Hospital, Sun Yat-sen University, Guangzhou, 510080, China
[f] Department of Radiotherapy, First Affiliated Hospital, Sun Yat-sen University, Guangzhou, 510080, China
[g] Department of General Surgery, First Affiliated Hospital, Sun Yat-sen University, Guangzhou, 510080, China
[h] Clinical Trials Unit, First Affiliated Hospital, Sun Yat-sen University, Guangzhou, 510080, China

ARTICLE INFO

Keywords:
Hepatocellular carcinoma
Incomplete radiofrequency ablation
Metastasis
Cancer stem cell
VEGFR1

ABSTRACT

Incomplete radiofrequency ablation (RFA) of hepatocellular carcinoma (HCC) could initiate malignant transition. Patient-derived xenograft (PDX) mice model was established to investigate the effect of VEGF pathway in incomplete RFA of HCC with high fidelity. Cancer stem cell markers and metastatic markers were increased after incomplete RFA, with increased VEGFR1 and decreased VEGFR2 expression. *In vitro* experiments revealed sublethal heat treatment promoted migration ability of HepG2, HCCLM3, and SMMC7721 cells, which coincided with enhanced ability of sphere formation and up-regulation of VEGFR1, CD133, CD44, and EpCAM. Moreover, HCC cells secreted more VEGF after heat-treatment. VEGF promoted migration and enhanced stemness of HCC cells, which could not be suppressed by VEGFR2 inhibitor. PIGF, the ligand of VEGFR1, significantly increased migration and stemness of HCC cells. Blocking VEGFR1 reduced heat-induced enhancement of migration and stemness, whereas inhibition of VEGFR2 could not. In conclusion, VEGFR1 plays a critical role in sublethal heat treatment-induced enhancement of migration and stemness in HCC, suggesting that VEGFR1 may serve as a potential and promising therapeutic target for preventing recurrence after RFA.

1. Introduction

Hepatocellular carcinoma (HCC) remains one of the most common and fatal malignancies in the world [1–3]. For very early and early stage HCC, ablation is recommended as one of the curative therapies [4–7]. Radiofrequency ablation (RFA) is the most widely used thermal ablation treatment [8–10]. However, approximately 50% of HCC patients recur within 3 years after RFA [11–13]. Intrahepatic metastasis still remains the major cause of treatment failure [14,15]. Despite of years of efforts, there is no significant advancement in preventing tumor recurrence due to the poor understanding of metastatic dissemination after RFA. The STORM trial aiming to assess the efficacy and safety of sorafenib in preventing HCC recurrence after resection or ablation failed to meet its primary endpoint of improving recurrence-free survival [16]. Besides, there still lacks sufficient evidence for other adjuvant therapies to improve outcomes after RFA.

Abbreviations: RFA, radiofrequency ablation; HCC, hepatocellular carcinoma; PDX, patient-derived xenograft; CSC, cancer stem cell; EpCAM, epithelial cell adhesion molecule; VEGF, vascular endothelial growth factor; VEGFR 1/2, vascular endothelial growth factor receptor 1/2; PIGF, placental growth factor; VEGFR1-NA, VEGFR1 neutralized antibody; MMP, matrix metalloproteinase; EMT, epithelial-mesenchymal transition; NADH, Nicotinamide Adenine Dinucleotide; FBS, fetal bovine serum; HIF, hypoxia-inducible factor; ELISA, Enzyme linked immunosorbent assay

* Corresponding author. Department of Liver Surgery, Division of Interventional Ultrasound, Precision Medicine Institute, The First Affiliated Hospital, Sun Yat-sen University, 58 Zhong Shan Road 2, Guangzhou, 510080, China.
** Corresponding author. Department of Oncology, Precision Medicine Institute, The First Affiliated Hospital, Sun Yat-sen University, 58 Zhong Shan Road 2, Guangzhou, 510080, China.
E-mail addresses: lixiaxu320@163.com (L. Xu), kuangm@mail.sysu.edu.cn (M. Kuang).
[1] The first three authors contributed equally to this work.

https://doi.org/10.1016/j.canlet.2019.05.041
Received 10 February 2019; Received in revised form 29 May 2019; Accepted 30 May 2019

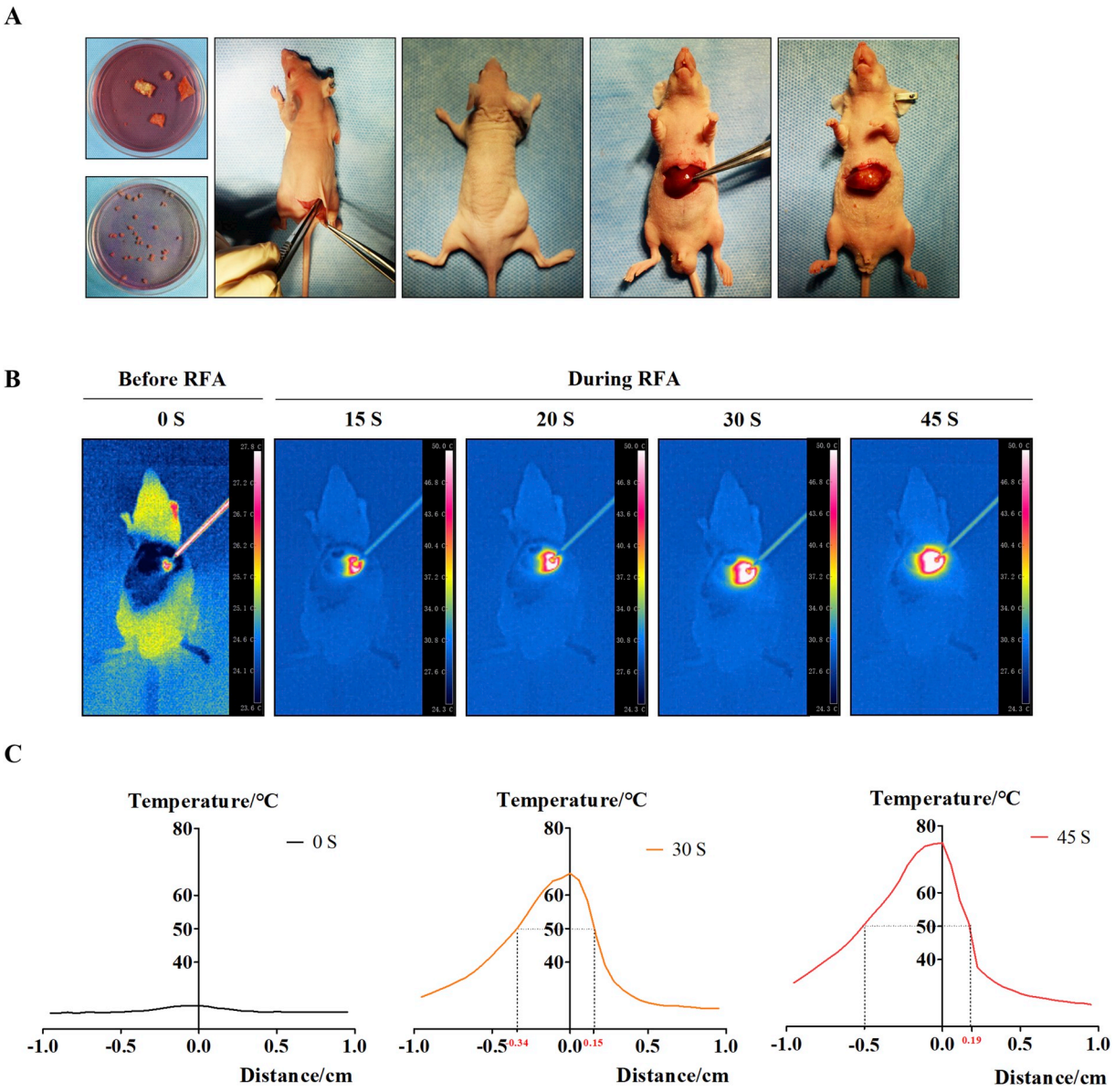

Fig. 1. Implementation of incomplete radiofrequency ablation (RFA) on patient-derived xenograft (PDX) mice. (A) HCC tumor tissues were obtained from surgical specimens. Tumor blocks were cut into pieces at 1 mm × 1 mm x 1 mm and implanted into right flank of mouse to form subcutaneous tumor. Subcutaneous tumor was then harvested and implanted into mouse liver to form orthotopic PDX. (B) Infrared imaging system was used to dynamically monitor thermal change during RFA. Longer ablation time would result in larger hyperthermic zone (> 50 °C) and higher central point temperature. (C) Infrared imaging data was further analyzed, demonstrating the relationship between distance and temperature during RFA. Asymmetry was caused by eccentric insertion of electrode.

It is reported that poor defined tumor margin may give rise to incomplete RFA [17,18], which could promote malignant transition of residual HCC due to sublethal heat treatment [19,20]. Further investigations reported that sublethal heat treatment could promote epithelial-mesenchymal transition (EMT) and enhance progenitor phenotype of HCC [21–23], which is indicated by the up-regulation of cancer stem cell (CSC) markers. The CSC refers to a special subpopulation in tumors which retains unattenuated capacity of tumor initiation and differentiation [24]. It is believed that CSC might be responsible for therapy resistance and tumor metastasis [25]. So far, some surface markers and functional tests have been reported to identify CSC in tumors. CD133, CD44, and EpCAM are regarded as important surface markers of CSC in HCC [26–28].

Vascular endothelial growth factor (VEGF), which is closely related to angiogenesis and vascular permeability, is now believed to contribute to tumorigenesis, especially CSC development [29,30]. Different VEGF receptors may be responsible for different physiological or pathological functions and are certainly variably expressed in varied tumors [29]. Previous studies have revealed that incomplete RFA of HCC could activate HIF/VEGF pathway to mediate malignant transition [21,22,31–33]. It has been reported that VEGF signaling pathway could enhance cancer stemness and renewal in skin cancer and glioblastoma multiforme [34,35]. We previously found the important role of autocrine VEGF pathway in HCC cell proliferation [36]. Thus, we hypothesize that VEGF signaling might play a role in incomplete RFA-related intrahepatic metastasis and stemness.

In this study, we explored the molecular alterations of residual HCC cells after incomplete RFA using simulation model of PDX and *in vitro* experiments, and investigated the role of VEGF and its receptors in incomplete RFA-related intrahepatic metastasis and stemness in HCC cells. Sublethal heat treatment could increase the migration capability and enhance stem cell-like phenotype of HCC cells through VEGF-VEGFR1 pathway.

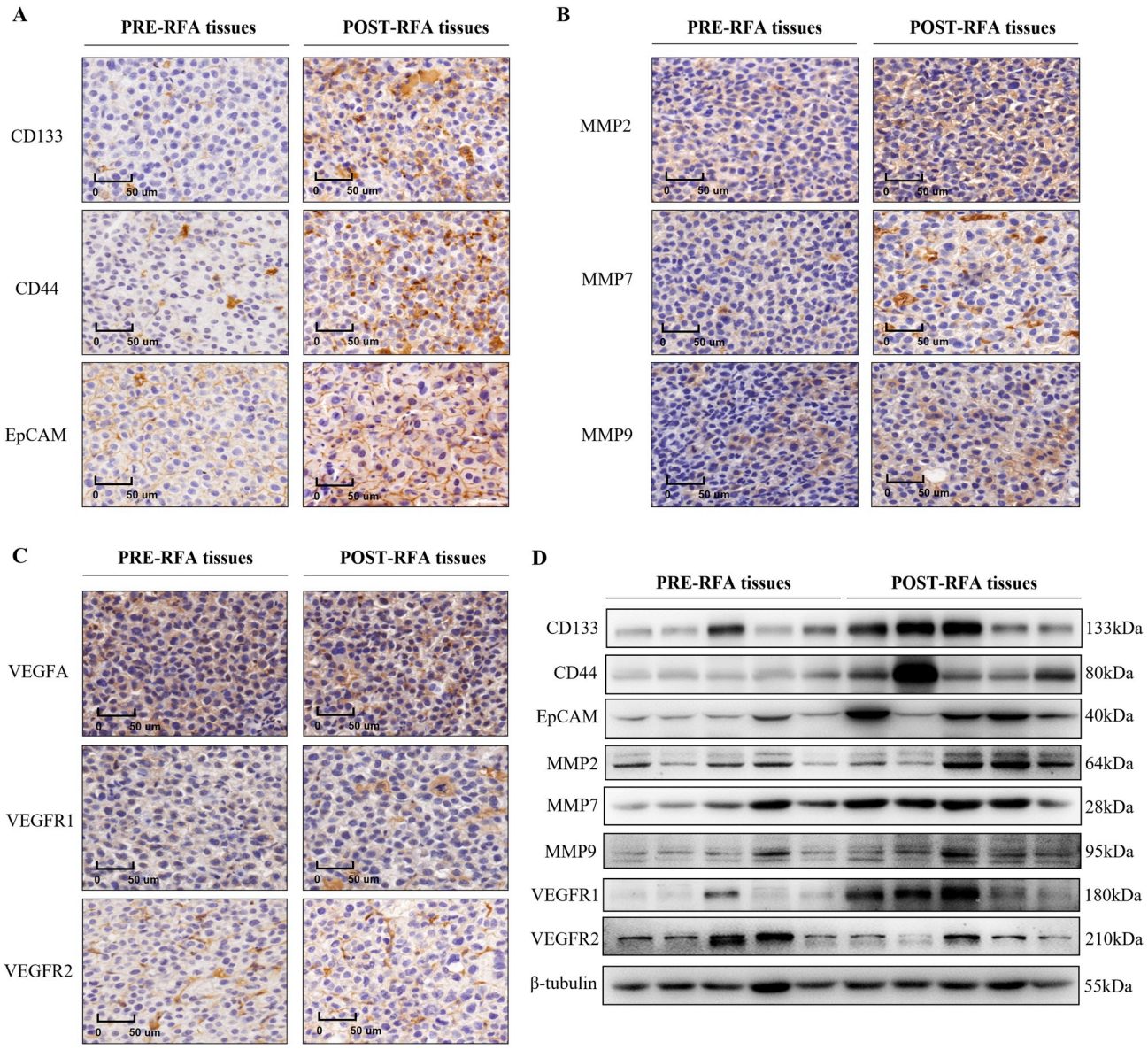

Fig. 2. Detection of cancer stem cell markers and metastatic markers in PDX after incomplete RFA. (A–C) Immunohistochemical staining was performed to evaluate expression of CD133, CD44, EpCAM, MMP2, MMP7, MMP9, VEGFA, VEGFR1 and VEGFR2 in tissues before and after RFA. Cancer stem cell markers and metastatic markers were up-regulated after incomplete RFA. VEGFA tended to be increased. And VEGFR1 was up-regulated while VEGFR2 was down-regulated. Magnifications were 200×. (D) Western blots were performed to confirm above molecular alterations.

2. Materials and methods

2.1. Patient-derived xenograft (PDX) model and incomplete RFA of HCC

HCC tumor tissues were obtained from surgical specimens. Patient-related projects have been authorized by the Institutional Review Board of the First Affiliated Hospital of Sun Yat-sen University (FAH-SYSU) according to the ethical guidelines of the 1975 Declaration of Helsinki. Informed Consent Forms have been collected from patients enrolled. Blood samples have also been collected from some patients before and after RFA. Male BALB/c (6 to 8-week-old) nude mice were purchased and housed with a 12-h light-dark cycle and permitted ad libitum consumption of water and a standard chow diet unless otherwise stated. All animal procedures were approved by Institutional Care and Animal Use Committee of FAH-SYSU according to the Reporting of *In Vivo* Experiments (ARRIVE) guidelines drafted by National Centre for the Replacement, Refinement and Reduction of Animals in Research (NC3Rs). Right after surgical resection, appropriate tissues were obtained and transferred in cold serum-free Dulbecco's modified Eagle's medium (DMEM; Gibco, Grand Island, NY, USA). After washing out of blood and unwanted tissues, the tumor blocks were cut into pieces at 1 mm × 1 mm x 1 mm under sterilized condition. Mice were anesthetized. And a 1 cm subcutaneous pocket was made on the right flank to store the tumor piece. About three months later, successful subcutaneous xenograft was visible and could be stably passed from one mouse to another. We anesthetized the tumor-bearing mice again to harvest the tumors and cut them into pieces at 1 mm × 1 mm x 1 mm again. Another batch of mice was anesthetized. Subcostal incision was performed to expose liver lobes. Tumor pieces were placed into the liver *via* a tunnel made by microscopic forceps. Mice were resumed feeding to nourish orthotopic tumor. Successful orthotopic tumor could be palpated within 2 months.

RFA devices includes VIVA RF generator, VIVA RF cool-tip electrode, VIVA grounding pad and VIVA pump (VRS01, STARmed, Gyeonggi-do, Korea). Orthotopic HCC tumor-bearing mice were anesthetized and put on the VIVA grounding pad. After exposing

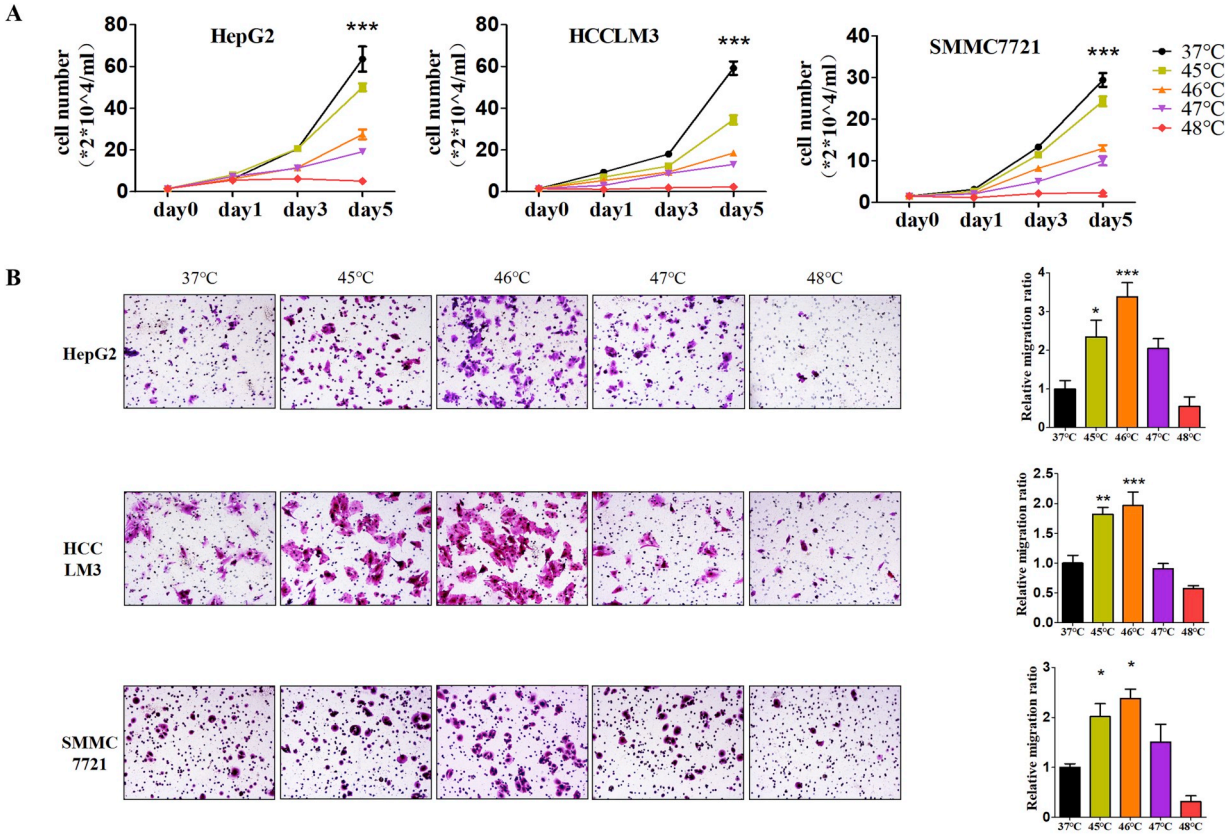

(caption on next page)

Fig. 3. The biological changes of HCC cells after heat treatment. (A) The cell number after heat treatment indicated that cell proliferative ability was decreased as the temperature increased. (B) Representative images of the migrated cells after heat treatment. Magnifications were 100×. Statistical analysis was performed (right). 46°C-treatment significantly increased the migration capacity. (C) Sublethal heat treatment increased the expression of MMP2, MMP7 and MMP9 in HCC. (D) Representative images of sphere formation after heat treatment. Magnifications were 50×. Statistical analysis was performed (right). 46°C-treatment significantly increased the ability of sphere formation. (E) Sublethal heat treatment increased the expression of CD133, CD44 and EpCAM in HCC. Data are displayed as mean ± SEM (n = 3–5). *$p < 0.05$; **$p < 0.01$; ***$p < 0.001$.

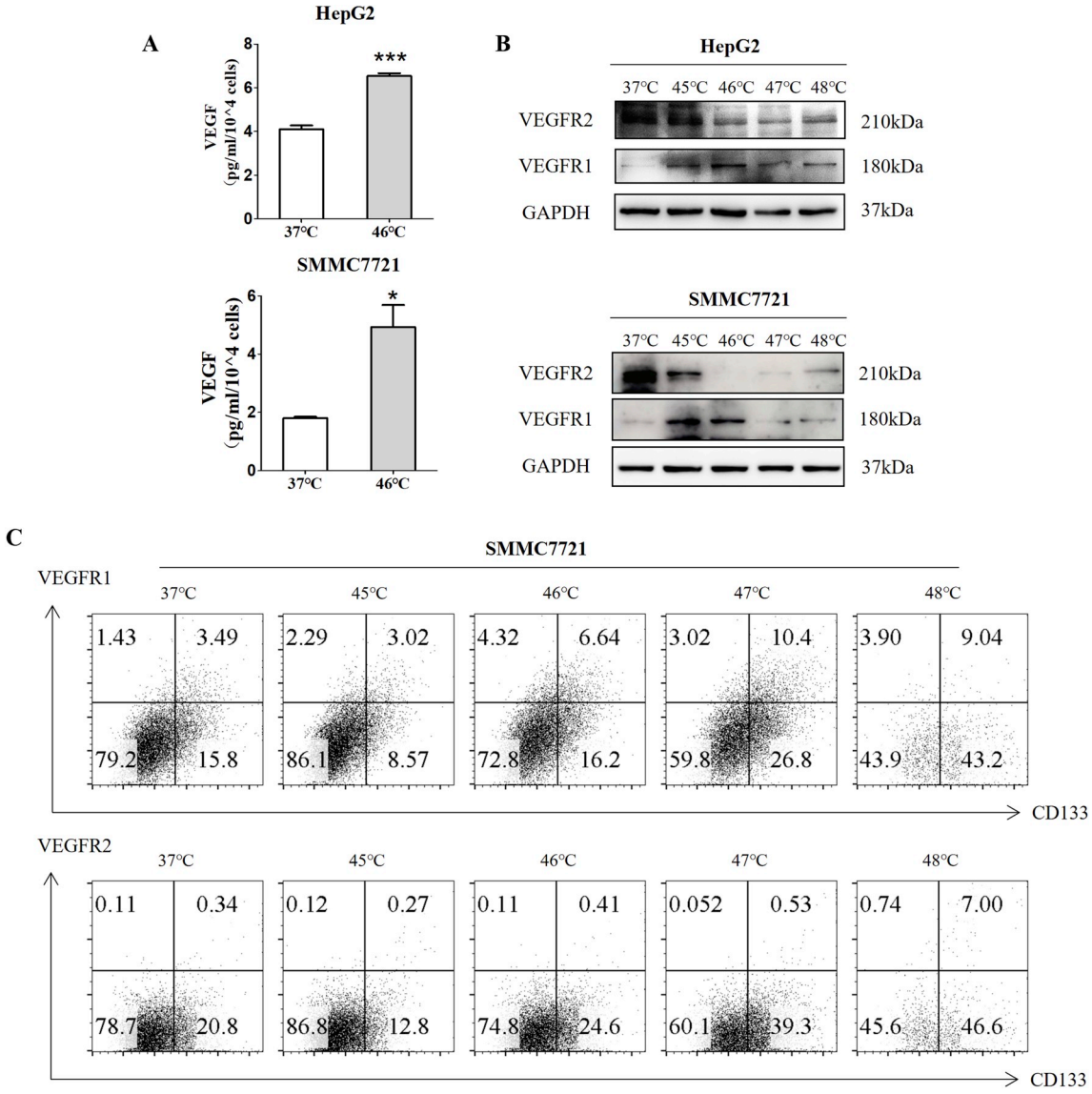

Fig. 4. Sublethal heat treatment promoted the secretion of VEGF, increased the expression of VEGFR1 and decreased the expression of VEGFR2. (A) ELISA was performed to measure the concentration of VEGF of culture supernatant 24 h after heat treatment. In particular, cells were counted at the time the supernatant were harvested, to calculate the concentration of VEGF per 10,000 cells. (B) After heat treatment, VEGFR1 were up-regulated and VEGFR2 were down-regulated. (C) The flow cytometry results showed that VEGFR1 was positively correlated with CD133. Data are displayed as mean ± SEM (n = 3). *$p < 0.05$; **$p < 0.01$; ***$p < 0.001$.

orthotopic tumor, we took a few tissues as the tumor tissues before RFA (Fig. 1A). Electrode was then inserted into the tumor eccentrically. To achieve accredited incomplete RFA, generator was set at 5 W for 30 s. An infrared camera (MAG32, Magnity Electronics Co. Ltd. Shanghai, China) was used to record dynamic thermal change (Fig. 1B–C). Seven days after RFA, orthotopic tumors were harvested for subsequent analyses, which would be compared with tumor tissues before RFA.

2.2. Nicotinamide Adenine Dinucleotide Diaphorase (NADH-diaphorase) staining

In order to validate the incomplete RFA of PDX-HCC, NADH-diaphorase staining was performed as previously described [37] to assess the viability of residual tumor tissues after RFA. The vital tumor cells would present with a purple staining, which is similar to positive control. All slides were reviewed by pathologists who were blinded to the research purpose.

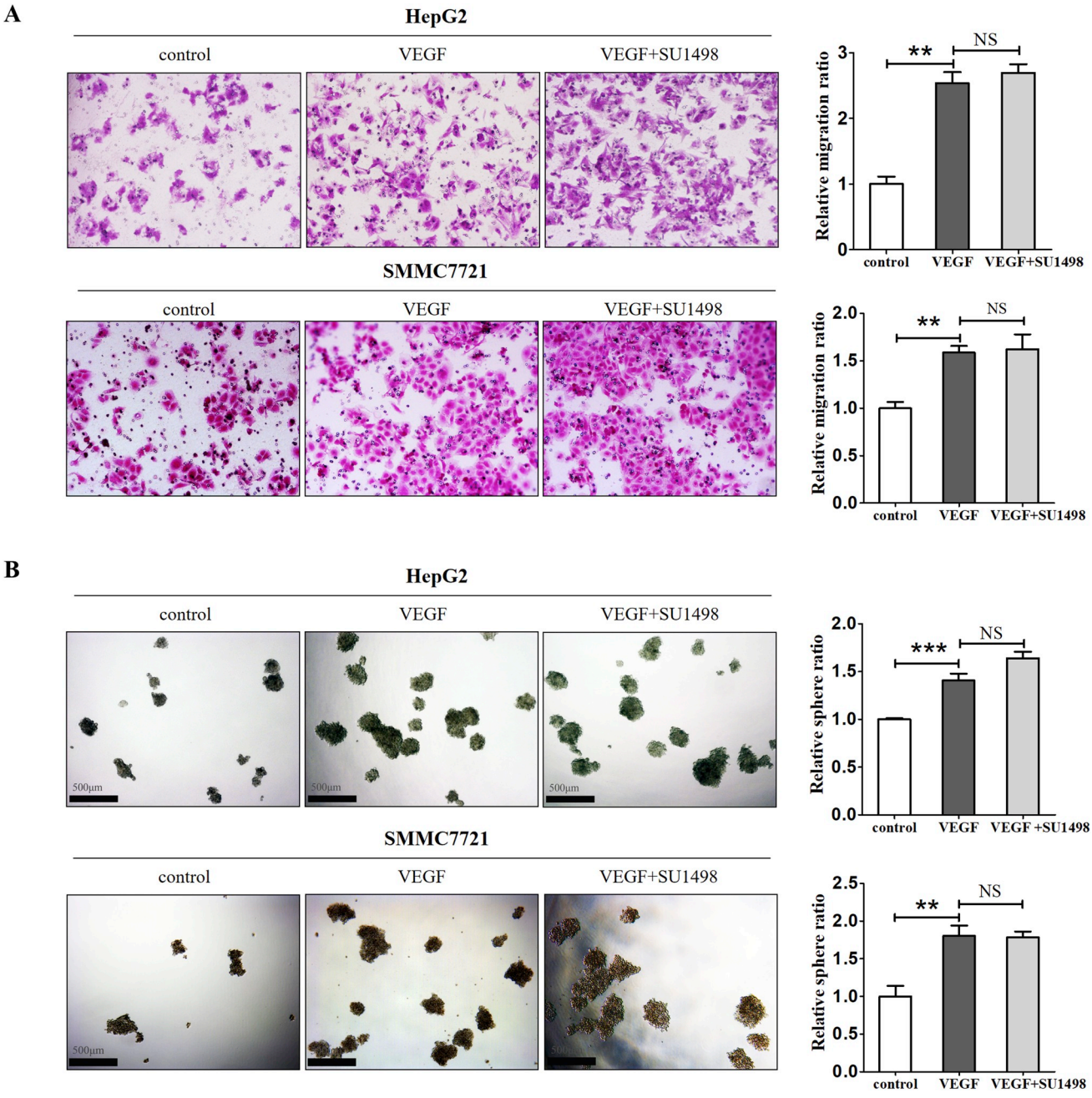

(caption on next page)

Fig. 5. VEGF increased the migration ability and stemness of HCC, which could not be repressed by inhibition of VEGFR2. (A) Representative images of the migrated cells after VEGF or VEGF plus SU1498 treatment. Magnifications were 100×. Statistical analysis was performed (right). VEGF can significantly increase the migration capacity. Additional treatment of SU1498 didn't reduce this effect but even increased it though not significantly. (B) Representative images of sphere formation. Magnifications were 50×. Statistical analysis was performed (right). VEGF treatment significantly increased the ability of sphere formation, which couldn't be reduced by SU1498. (C) VEGF stimulation up-regulated the expression of EpCAM, CD133 and CD44. Additional inhibition of VEGFR2 by SU1498 could not repress this effect. Data are displayed as mean ± SEM (n = 5), and are expressed as relative ratio using control group as the reference. $*p < 0.05$; $**p < 0.01$; $***p < 0.001$.

2.3. Immunohistochemistry (IHC)

Tissues embedded in paraffin were sectioned into 4 μm slides. After incubated with corresponding antibodies (Supplementary Table 2), slides were treated with envision system and DAB-chromogen, which was followed with counterstaining of hematoxylin. Results were reviewed by pathologists who were blinded to the research purpose.

2.4. Cell lines and sublethal heat treatment

HCC cell lines HepG2, HCCLM3 and SMMC7721 were obtained from Cell Bank of Chinese Academy of Medical Science (Shanghai, China). HepG2 and HCCLM3 were cultured in DMEM (Gibco, Grand Island, NY, USA) containing 10% fetal bovine serum (FBS, Invitrogen Life Technology, Carlsbad, CA), 100 IU/ml penicillin and 100 μg/ml streptomycin. SMMC7721 were cultured in RPMI-1640 (Gibco, Grand Island, NY, USA), supplemented with 10% FBS (Invitrogen Life Technology, Carlsbad, CA), 100 U/ml penicillin and 100 μg/ml streptomycin. Accordingly, cells grown to 70%–80% confluence were starved with 1% FBS supplemented DMEM or RPMI-1640 for 12 h s and were exposed to different temperature heat treatments for 10 min a water-bath way. Medium was changed to fresh 10% FBS supplemented DMEM or RPMI-1640 after the heat treatment. Cells were then cultured for subsequent research.

2.5. Cell counting and transwell assay

HCC cells were trypsinized and re-plated into 6-well plates with 30,000 cells per well 24 h after heat treatment, and were incubated with the medium described above. Cells were collected and counted using automated cell counter (ALIT Life Science, Shanghai, China) at day 1, 3 and 5 after plating. Transwell assay was performed as previously described [38]. Images were captured using inverted microscope equipped with an Olympus Qcolor 3 digital camera (Zeiss, Oberkochen, Germany). Five fields of 100x magnification for each well were randomly selected for statistical calculation.

2.6. Western blot

After treatment, cells or tissues were harvested, and protein extracts were prepared on ice using cold RIPA buffer. 20 μg proteins were electrophoresed in 8% sodium dodecyl sulfate–polyacrylamide gel electrophoresis (SDS-PAGE), and blotted onto PVDF membranes (Millipore, Billerica, MA, USA). Signals were determined by Western blotting using primary antibodies (Supplementary Table 1), followed by corresponding peroxidase-conjugated secondary antibodies and Immobilion Western Chemilum HRP Substrate (Millipore, Billerica, MA, USA).

2.7. Enzyme linked immunosorbent assay (ELISA)

HCC cells were seeded into 6-well plate with 500,000 cells per well. Heat-treatment was performed as described above. And 24 h later, the supernatant was collected for detection of VEGF and PIGF using ELISA kit (#KHG0112, Thermo Fisher Scientific, Waltham, MA, USA) (#ab100629, Abcam, Cambridge, MA, USA). Moreover, cells were counted at the same time, to calculate the concentration of VEGF produced by 10,000 cells. Patients' serums were also analyzed using ELISA kits above.

2.8. Flow cytometry

Three days after heat treatment, HCC cells were collected and re-suspended in PBS. Cells were then incubated with primary antibodies (Supplementary Table 1) at 4 °C for 30 min. The percentage of positive cells was detected using CytoFLEX (Beckman Coulter, Miami, FL, USA).

2.9. Sphere formation assay

After corresponding treatments, HCC cells were seeded into 96-well, ultra-low-attachment plates (Corning, New York, USA) with 300 cells per well. Cells were cultured in the standard sphere-forming medium for 7–10 days [39,40]. Spheres were captured at 50x magnification using inverted microscope. And spheres larger than 50 μm were counted for statistical analysis.

2.10. Application of VEGF, SU1498, PIGF and VEGFR1-neutralized antibody

Recombinant human VEGF (rhVEGF) (#293VE, R&D Systems, Minneapolis, MN, USA; 30 ng/ml) was added into culture medium to stimulate VEGFR1/2. SU1498 (#SML1193, Sigma-Aldrich, St. Louis, MO, USA; 10 μmol/ml) was used to inhibit VEGFR2. PIGF (#264PGB, R &D Systems, Minneapolis, MN, USA; 30 ng/ml) was used to stimulate VEGFR1. VEGFR1-neutrolized antibody (#AF321, R&D Systems, Minneapolis, MN, USA; 10 μg/ml) was used to block VEGFR1. To note, neutralized antibody should be added 30 min before the use of PIGF.

2.11. Statistical analysis

The SPSS software v18.0 (SPSS Inc, Chicago, IL) was used for statistical analysis. Quantitative data are presented as the means ± standard error of the mean (SEM). Comparisons were performed using one-way analysis of variance (one-way ANOVA), two-way analysis of variance (two-way ANOVA) or unpaired Student's t-test. A P-value less than 0.05 was considered as statistically significant.

3. Results

3.1. Incomplete RFA of PDX induced malignant transition of HCC and changed the profile of VEGF pathway

A batch of five orthotopic PDX mice was established for incomplete RFA (Fig. 1A). Infrared imaging system was used to monitor thermal change in this process. As illustrated in Fig. 1B–C and Supplementary Fig. 1A, certain heat effect was produced by electrode and was conducted from central to peripheral zones during RFA. Longer ablation time would dynamically result in larger hyperthermic zone (> 50 °C) and higher central point temperature. To achieve incomplete RFA and protect mice from overheat, we optimized ablation time to 30 s. Under such circumstance, our residual tumor samples which came from the edge of necrotic area (about 0.5 cm away from ablation centre) may suffer from a heat ranging from 40 °C to 50 °C for 30 s during RFA (Supplementary Fig. 1B and C). NADH-diaphorase staining was

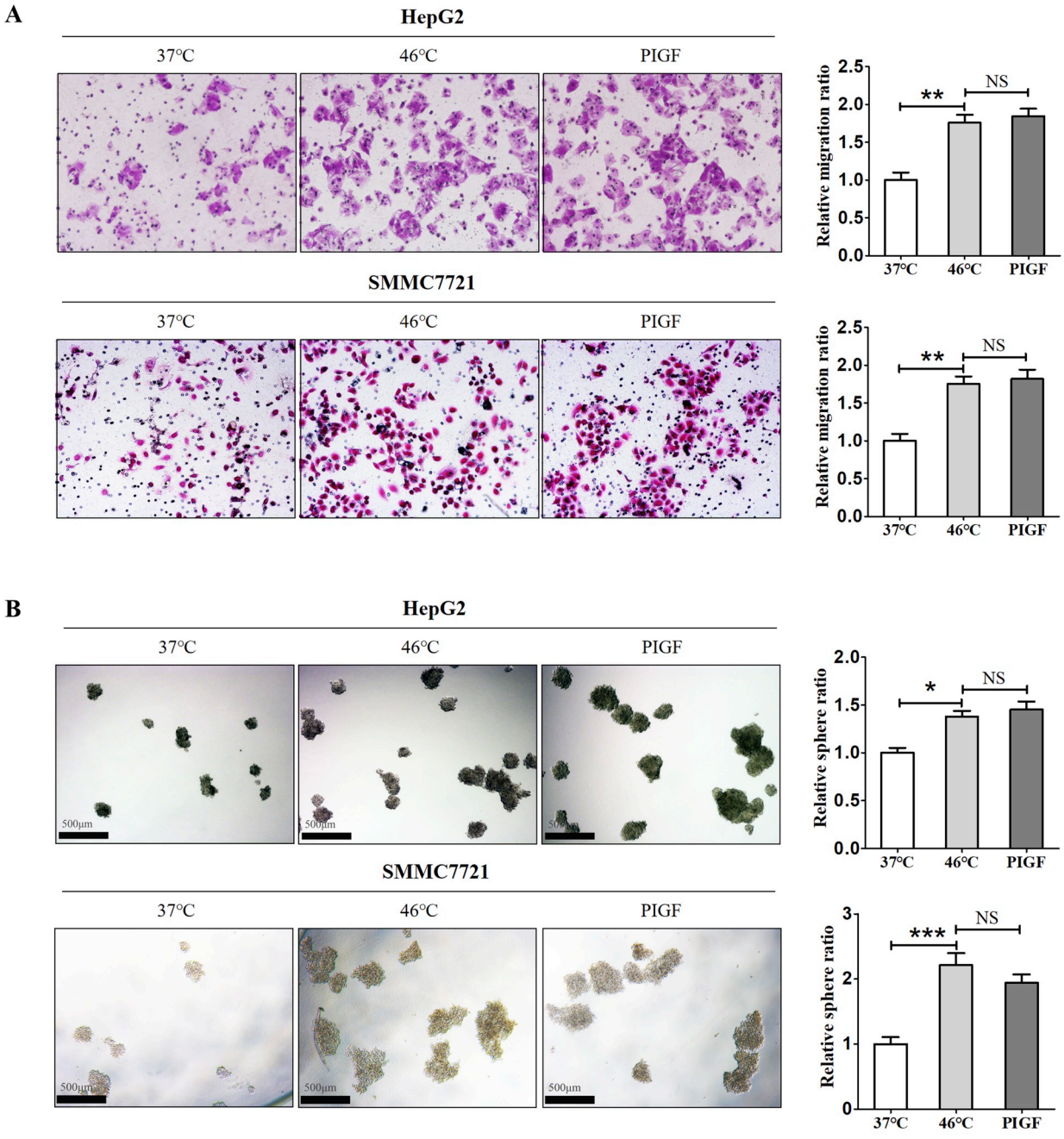

(caption on next page)

Fig. 6. Activation of VEGFR1 by PIGF increased the migration and stemness of HCC, which was similar to sublethal heat treatment. (A) Representative images of the migrated cells after 46 °C treatment and PIGF treatment. Magnifications were 100×. Statistical analysis was performed (right). PIGF increased the migration capacity as 46°C-treatment did. (B) Representative images of sphere formation. Magnifications were 50×. Statistical analysis was performed (right). Activation of VEGFR1 specifically increased the ability of sphere formation, which was similar to sublethal heat treatment. (C) PIGF increased the expression of EpCAM, CD133 and CD44, displaying a similar effect of 46°C-treatment. Data are displayed as mean ± SEM (n = 5), and are expressed as relative ratio using 37 °C treatment group as the reference. *$p < 0.05$; **$p < 0.01$; ***$p < 0.001$.

performed to validate incomplete RFA (Supplementary Fig. 2A).

Immunohistochemistry was used to detect in situ expression of CD133, CD44 and EpCAM before and after ablation (Fig. 2A). We also determined the expression of MMPs (Fig. 2B), which could hydrolyze the components of tumor matrix and pave the way for tumor invasion and migration [41]. Results revealed that incomplete RFA enhanced cancer stemness and metastatic potential in tumor cells, which was further confirmed by Western blot (Fig. 2D, Supplementary Fig. 2B).

With the aim to explore the role of VEGF pathway in such malignant transition, we detected VEGF and its main receptors using IHC and Western blot. Intriguingly, besides the increase of VEGF, we found VEGFR1 was up-regulated after incomplete RFA, while VEGFR2 was down-regulated (Fig. 2C–D, Supplementary Fig. 2B).

3.2. Sublethal heat treatment enhanced the metastatic potential of HCC cells

In vitro heat treatment model was applied to verify metastatic molecular changes. Unlike *in vivo* RFA in mice, specific temperature could be maintained in water bath. Thus, HepG2, HCCLM3 and SMMC7721 cells were heated with different temperature for 10 min, which is in accordance with most previous reports [23] and clinical operations. We found that heat treated cells showed decreased proliferative ability when compared to cells treated with 37 °C (Fig. 3A). Hyperthermia induced prolonged growth suppression. But a portion of cells did recover and continue to grow except for 48 °C heated cells. Those sublethal heated cells exhibited increased migration ability and higher expression of MMPs (Fig. 3B–C). Further statistical analysis indicated 46 °C was the most optimal temperature which exhibited the most significant migration-promoting effect of HCC cells.

3.3. Sublethal heat treatment promoted stem-cell like phenotype

We further evaluated the stem cell-like phenotypes of HCC cells after heat treatment. Through sphere formation assay, 46 °C heat treatment resulted in significant enhancement of stemness of HepG2, HCCLM3 and SMMC7721 cells (Fig. 3D). CD133, CD44, and EpCAM were markedly up-regulated in sublethal heat treated cells as determined *via* Western blot (Fig. 3E), which was further confirmed by flow cytometry (Supplementary Fig. 3).

3.4. HCC cells secreted more VEGF after sublethal heat treatment, along with up-regulation of VEGFR1

To confirm the alterations of VEGF and VEGFR1/2 *in vitro*, we detected the expression of these molecules in HCC cells. ELISA results showed increased VEGF secretion after sublethal heating (Fig. 4A). VEGFR1 was found to be up-regulated along with enhanced migration after heating while VEGFR2 was down-regulated by Western blot (Fig. 4B), which is consistent with the findings in PDX mice.

To further characterize the relationship between VEGFR1/2 and stemness, flow cytometry was carried out to analyze the correlation between VEGFR1/2 and CD133. Results showed that VEGFR1 was positively correlated with CD133 in the same cell population after heat treatment, whereas there was no correlation between VEGFR2 and CD133 (Fig. 4C).

3.5. VEGFR1 mediated the process of stemness and migration enhancement after sublethal heat treatment

To delineate the possible role of VEGF pathway alterations in malignant transition after sublethal heat treatment, extra reagents were used to stimulate or inhibit specific molecules. As expected, VEGF treatment enhanced cell migration and sphere formation ability, and up-regulated CSC markers as compared with control group (Fig. 5A–C). However, VEGFR2-specific inhibitor SU1498 could not suppress the effect of VEGF in HCC cell migration and stemness (Fig. 5A–C). It seemed that inhibiting VEGFR2 even enhanced this effect though not significant.

To further determine the role of VEGFR1 in malignant transition of HCC cells after sublethal heat treatment, cells were treated with VEGFR1-specific ligand PIGF, which could bind to and activate VEGFR1 specifically. We then found PIGF significantly promoted metastatic potential of HCC and enhanced stemness when compared with control group (Fig. 6A–C). The effect of PIGF treatment was similar to that of 46 °C heat treatment (Fig. 6A–C).

On the other hand, VEGFR1 neutralized antibody (VEGFR1-NA) was used to block VEGF-VEGFR1 pathway. Although the application of VEGFR1 neutralized antibody alone failed to suppress the metastasis and stemness significantly as compared with control group, the combination of VEGFR1 neutralized antibody with PIGF led to a significant decrease of metastatic capability and stemness as compared with PIGF group (Fig. 7).

Moreover, inhibition of VEGFR2 did not reduce the increased metastatic capability and stemness induced by sublethal heat treatment (Supplementary Figs. 4A–C). Nevertheless, VEGFR1-NA could significantly suppress the enhanced metastatic potential and stemness induced by sublethal heat treatment (Supplementary Figs. 5 and 6). Considering the effect of VEGF and VEGFR1 during sublethal heat treatment, we performed clinical validation using serum from HCC patients before and after RFA. Serum VEGF tended to be elevated after RFA in clinical patients although not significantly (Supplementary Fig. 7), which may be caused by small sample size and individual variation. However, PIGF serum level was proven to be significantly elevated after RFA, which was further confirmed in HepG2 cells after sublethal heating (Supplementary Fig. 7).

4. Discussion

HCC patients suffer from high recurrence rate after RFA. Local invasion and intrahepatic metastasis are reported to be related to incomplete RFA. Although increasing studies have attempted to elucidate the possible underlying mechanism, there is no solid supporting evidence for adjuvant therapy to prevent tumor relapse. Cancer stem cell was initially discovered in haemopoietic cancer [24]. It is well documented that CSCs can survive from the treatment and re-create the tumor away from the primary lesion [42]. Previous studies suggested the progenitor transition after heat treatment and the potential effect of VEGF signaling in this process [23,32,33]. However, the impact of VEGF receptors on tumor metastatic dissemination and tumor stemness remains obscure.

For translational medicine researches, fidelity should be a highlighted issue. However, very few tumor tissues can be obtained during RFA. Insufficient clinical resources give rise to bias view when we explore the driving mechanism of metastasis and recurrence after RFA. In

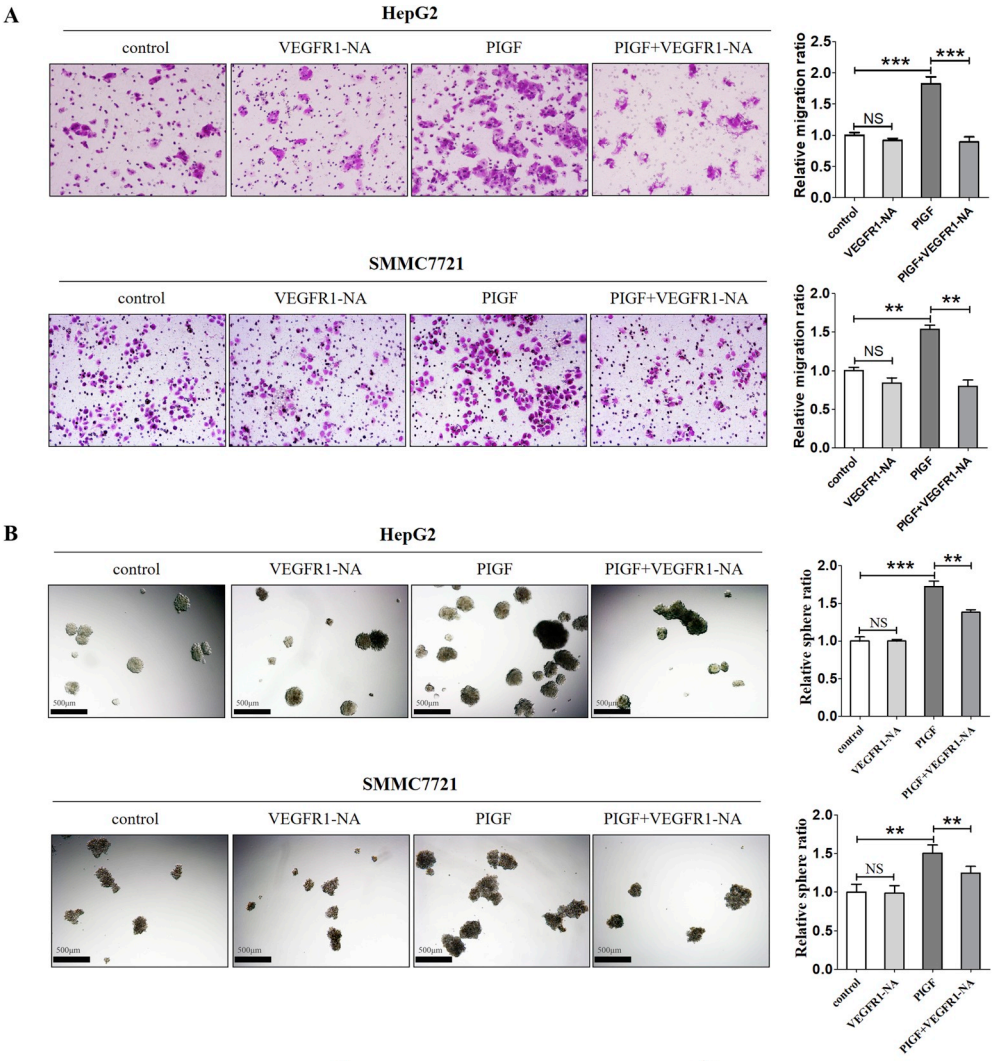

Fig. 7. Blocking VEGFR1 reduced metastatic ability and cancer stemness of HCC cells induced by PIGF. (A) Representative images of the migrated cells. Magnifications were 100×. Statistical analysis was performed (right). Additional blocking VEGFR1 decreased the migration ability induced by PIGF. As compared with control group, blocking VEGFR1 alone did not repress cell migration significantly. (B) Representative images of sphere formation. Magnifications were 50×. Statistical analysis was performed (right). Blocking VEGFR1 decreased the ability of sphere formation induced by PIGF. (C) Blocking VEGFR1 by VEGFR1-NA decreased the expression of MMP2, MMP7, MMP9 induced by PIGF treatment. (D) Blocking VEGFR1 by VEGFR1-NA decreased the expression of CD133, CD44 and EpCAM induced by PIGF treatment. Data are displayed as mean ± SEM (n = 5), and are expressed as relative ratio using 37 °C treatment group as the reference. *$p < 0.05$; **$p < 0.01$; ***$p < 0.001$.

this study, incomplete RFA model was established on HCC-PDX mice for the first time, to provide valuable information from clinical samples without ethical concerns. Through this model, we found increased expression of CSC markers and metastasis related markers in clinical samples after incomplete RFA. Meanwhile, VEGF receptors demonstrated an interesting transition. VEGFR2 is generally accepted as the predominant contributor to VEGF signaling but was down-regulated after incomplete RFA in our study, whereas VEGFR1 was up-regulated.

Hyperthermic injury is thought to be the common major tumor-killing effect during RFA [8]. However, temperature would decrease as the heat flows from the central area to peripheral zone. It's believed that, although RFA can produce over 50°C-heat effect in central zone, temperature will be reduced to 41°C–45 °C in the adjacent area [43]. Such temperature may be not able to kill the tumor cells but rather promote the malignancy. We used infrared imaging system to detect thermal change during incomplete RFA on PDX. Results showed that, at the edge of necrotic area, heating ranging from 40 °C to 50 °C for 30 s would initiate malignant transition and alter the profile of VEGF pathway. Subsequent investigations in HCC cell lines also confirmed the similar molecular alterations induced by sublethal heat treatment. To specify the unique effect of VEGFR1 increased by heat treatment, additional reagents were applied to activate or inhibit VEGFR1/2. We then found that inhibition of VEGFR2 could not interrupt VEGF-promoting tumor migration and stemness. But VEGFR1 could mediate increased metastatic phenotype of HCC. And blocking VEGFR1 can alleviate heat-induced malignancy, implying that VEGFR1 might serve as a therapeutic target for preventing recurrence after RFA.

Thermal ablation should have a promising application future due to a variety of advantages [8]. However, heat-induced malignant transition remains the major obstacle. Our study demonstrated the intriguing molecular alterations induced by sublethal heat and provided a possible target for recurrence prevention. But there are still some limitations in our study. Due to the property of murine model, heat is reduced to achieve incomplete RFA on PDX mice, but the temperature and duration time are certainly different between clinical situation and *in vitro* experiments although it did promote malignant transition. And limited by PDX mice resources we have, the targetable role of VEGFR1 has not been validated *in vivo*. Further investigations should be followed using PDX mice derived from more patients. Also, although we tried to verify our results using clinical serum samples, further large-scale clinical validations are needed.

Moreover, we noted that inhibition of VEGFR2 could even increase the malignant transition though not significantly. It has been reported that the heterodimerization of VEGFR1/2 can regulate the cell homeostasis [44]. Further investigations are required to explore the causal relationship between heat and VEGFR1, and the effect of VEGFR1/2 dimerization.

In conclusion, sublethal heat treatment can activate VEGF pathway and alter VEGFRs profile, which enhances metastatic potential and cancer stemness of HCC cells *via* a VEGFR1-dependent manner. Our data suggests VEGFR1 as a potential and promising therapeutic target for preventing recurrence after RFA.

Conflicts of interest

The authors declare that they have no conflict of interest.

Authors contributions

Ming Kuang and Lixia Xu conceived and designed the study. Li Tan, Shuling Chen, Huilin Jin and Junbin Liao performed the animal experiments. Li Tan, Guangyan Wei, Yue Li, Ying Zou and Manling Huang performed the *in vitro* experiments. Li Tan, Guangyan Wei collected the data. Shuling Chen performed the data analysis and interpretation. Li Tan, Guangyan Wei wrote the initial draft. Sui Peng, Zhenwei Peng and Yu Guo helped review and edit manuscript. Li Tan, Lixia Xu and Ming Kuang wrote the final report. All authors contributed to critical revision of the final report. Lixia Xu and Ming Kuang are guarantors. All the authors had full access to all of the data and can take responsibility for the integrity of the data and the accuracy of the data analysis.

Acknowledgement

This study was supported by the National Natural Science Foundation of China for Distinguished Young Scholar of China (No. 81825013); National Natural Science Foundation of China (No. 81771958); Science and Technology Program of Guangzhou, China (No. 201704020099); Science and Technology Program of Guangzhou, China (No. 201704020215); National Natural Science Foundation of China (No. 81801703).

Appendix A. Supplementary data

Supplementary data to this article can be found online at https://doi.org/10.1016/j.canlet.2019.05.041.

References

[1] F. Bray, et al., Global cancer statistics 2018: GLOBOCAN estimates of incidence and mortality worldwide for 36 cancers in 185 countries, CA A Cancer J. Clin. 68 (6) (2018) 394–424.
[2] Global, B.O.D.C., et al., Global, regional, and national cancer incidence, mortality, years of life lost, years lived with disability, and disability-adjusted life-years for 29 cancer groups, 1990 to 2016: A systematic analysis for the global burden of disease study, JAMA Oncol. 4 (11) (2018) 1553–1568.
[3] W. Chen, R. Zheng, P.D. Baade, S. Zhang, H. Zeng, F. Bray, et al., Cancer statistics in China, 2015, CA: Cancer J. Clin. 66 (2016) 115–132.
[4] J. Llovet, C.J. Bru, Prognosis of hepatocellular carcinoma: the BCLC staging classification, Semin. Liver Dis. 19 (1999) 329–338.
[5] J. Bruix, M. Reig, M. Sherman, Evidence-based diagnosis, staging, and treatment of patients with hepatocellular carcinoma, Gastroenterology 150 (2016) 835–853.
[6] P.R. Galle, A. Forner, J.M. Llovet, V. Mazzaferro, F. Piscaglia, J. Raoul, et al., EASL clinical practice guidelines: management of hepatocellular carcinoma, J. Hepatol. 69 (2018) 182–236.
[7] J.A. Marrero, L.M. Kulik, C.B. Sirlin, A.X. Zhu, R.S. Finn, M.M. Abecassis, et al., Diagnosis, staging, and management of hepatocellular carcinoma: 2018 practice guidance by the American association for the study of liver diseases, Hepatology 68 (2018) 723–750.
[8] K.F. Chu, D.E. Dupuy, Thermal ablation of tumours: biological mechanisms and advances in therapy, Nat. Rev. Canc. 14 (2014) 199–208.
[9] R. Lencioni, L. Crocetti, Local-regional treatment of hepatocellular carcinoma, Radiology 262 (2012) 43–58.
[10] Y.K. Cho, J.K. Kim, M.Y. Kim, H. Rhim, J.K. Han, Systematic review of randomized trials for hepatocellular carcinoma treated with percutaneous ablation therapies, Hepatology 49 (2009) 453–459.
[11] D.H. Lee, J.M. Lee, J.Y. Lee, S.H. Kim, J.H. Yoon, Y.J. Kim, et al., Radiofrequency ablation of hepatocellular carcinoma as first-line treatment: long-term results and prognostic factors in 162 patients with cirrhosis, Radiology 270 (2014) 900–909.
[12] A. Cucchetti, F. Piscaglia, M. Cescon, A. Colecchia, G. Ercolani, L. Bolondi, et al., Cost-effectiveness of hepatic resection versus percutaneous radiofrequency ablation for early hepatocellular carcinoma, J. Hepatol. 59 (2013) 300–307.
[13] R. Lencioni, D. Cioni, L. Crocetti, C. Franchini, C.D. Pina, J. Lera, et al., Early-stage hepatocellular carcinoma in patients with cirrhosis: long-term results of percutaneous image-guided radiofrequency ablation, Radiology 234 (2005) 961–967.
[14] D. Choi, H.K. Lim, H. Rhim, Y. Kim, W.J. Lee, S.W. Paik, et al., Percutaneous radiofrequency ablation for early-stage hepatocellular carcinoma as a first-line treatment: long-term results and prognostic factors in a large single-institution series, Eur. Radiol. 17 (2007) 684–692.
[15] S. Rossi, V. Ravetta, L. Rosa, G. Ghittoni, F.T. Viera, F. Garbagnati, et al., Repeated radiofrequency ablation for management of patients with cirrhosis with small hepatocellular carcinomas: a long-term cohort study, Hepatology 53 (2011) 136–147.
[16] J.P. Bruix, T.P. Takayama, V.P. Mazzaferro, G.P. Chau, J.P. Yang, M.P. Kudo, et al., Adjuvant sorafenib for hepatocellular carcinoma after resection or ablation (STORM): a phase 3, randomised, double-blind, placebo-controlled trial, Lancet Oncol. 16 (2015) 1344–1354.
[17] S.A. Curley, F. Izzo, P. Delrio, L.M. Ellis, J. Granchi, P. Vallone, et al., Radiofrequency ablation of unresectable primary and metastatic hepatic malignancies: results in 123 patients, Ann. Surg. 230 (1999) 1–8.
[18] V. Mazzaferro, R. Lencioni, P. Majno, Early hepatocellular carcinoma on the procrustean bed of ablation, resection, and transplantation, Semin. Liver Dis. 34 (2014) 415–426.
[19] R. Zhang, M. Ma, X. Lin, H. Liu, J. Chen, J. Chen, et al., Extracellular matrix collagen I promotes the tumor progression of residual hepatocellular carcinoma after heat treatment, BMC Canc. 18 (2018).
[20] Z. Zhao, J. Wu, X. Liu, M. Liang, X. Zhou, S. Ouyang, et al., Insufficient

radiofrequency ablation promotes proliferation of residual hepatocellular carcinoma via autophagy, Cancer Lett. 421 (2018) 73–81.
[21] S. Iwahashi, M. Shimada, T. Utsunomiya, S. Imura, Y. Morine, T. Ikemoto, et al., Epithelial–mesenchymal transition-related genes are linked to aggressive local recurrence of hepatocellular carcinoma after radiofrequency ablation, Cancer Lett. 375 (2016) 47–50.
[22] S. Yamada, T. Utsunomiya, Y. Morine, S. Imura, T. Ikemoto, Y. Arakawa, et al., Expressions of hypoxia-inducible factor-1 and epithelial cell adhesion molecule are linked with aggressive local recurrence of hepatocellular carcinoma after radiofrequency ablation therapy, Ann. Surg. Oncol. 21 (2014) 436–442.
[23] S. Yoshida, M. Kornek, N. Ikenaga, M. Schmelzle, R. Masuzaki, E. Csizmadia, et al., Sublethal heat treatment promotes epithelial-mesenchymal transition and enhances the malignant potential of hepatocellular carcinoma, Hepatology 58 (2013) 1667–1680.
[24] T. Reya, S.J. Morrison, M.F. Clarke, I.L. Weissman, Stem cells, cancer, and cancer stem cells, Nature 414 (2001) 105.
[25] J.E. Visvader, G.J. Lindeman, Cancer stem cells in solid tumours: accumulating evidence and unresolved questions, Nat. Rev. Canc. 8 (2008) 755.
[26] J. Sun, Q. Luo, L. Liu, G. Song, Liver cancer stem cell markers: progression and therapeutic implications, World J. Gastroenterol. 22 (2016) 3547.
[27] J. Jang, Y. Song, S. Kim, J. Kim, K.M. Kim, E.K. Choi, et al., CD133 confers cancer stem-like cell properties by stabilizing EGFR-AKT signaling in hepatocellular carcinoma, Cancer Lett. 389 (2017) 1–10.
[28] H. You, W. Ding, H. Dang, Y. Jiang, C.B. Rountree, c-Met represents a potential therapeutic target for personalized treatment in hepatocellular carcinoma, Hepatology 54 (2011) 879–889.
[29] H.L. Goel, A.M. Mercurio, VEGF targets the tumour cell, Nat. Rev. Canc. 13 (2013) 871–882.
[30] D. Zhao, C. Pan, J. Sun, C. Gilbert, K. Drews-Elger, D.J. Azzam, et al., VEGF drives cancer-initiating stem cells through VEGFR-2/Stat3 signaling to upregulate Myc and Sox2, Oncogene 34 (2014) 3107.
[31] Y. Tong, H. Yang, X. Xu, J. Ruan, M. Liang, J. Wu, et al., Effect of a hypoxic microenvironment after radiofrequency ablation on residual hepatocellular cell migration and invasion, Cancer Sci. 108 (2017) 753–762.
[32] R.T.P. Poon, C. Lau, R. Pang, K.K. Ng, J. Yuen, S.T. Fan, High serum vascular endothelial growth factor levels predict poor prognosis after radiofrequency ablation of hepatocellular carcinoma: importance of tumor biomarker in ablative therapies, Ann. Surg. Oncol. 14 (2007) 1835–1845.
[33] Z. Liu, H. Dai, G. Jia, Y. Li, X. Liu, W. Ren, Insufficient radiofrequency ablation promotes human hepatoma SMMC7721 cell proliferation by stimulating vascular endothelial growth factor overexpression, Oncol. Lett. 9 (2015) 1893–1896.
[34] P. Hamerlik, J.D. Lathia, R. Rasmussen, Q. Wu, J. Bartkova, M. Lee, et al., Autocrine VEGF–VEGFR2–Neuropilin-1 signaling promotes glioma stem-like cell viability and tumor growth, J. Exp. Med. 209 (2012) 507–520.
[35] B. Beck, G. Driessens, S. Goossens, K.K. Youssef, A. Kuchnio, A. Caauwe, et al., A vascular niche and a VEGF–Nrp1 loop regulate the initiation and stemness of skin tumours, Nature 478 (2011) 399–403.
[36] S. Peng, Y. Wang, H. Peng, D. Chen, S. Shen, B. Peng, et al., Autocrine vascular endothelial growth factor signaling promotes cell proliferation and modulates sorafenib treatment efficacy in hepatocellular carcinoma, Hepatology 60 (2014) 1264–1277.
[37] M. Nikfarjam, V. Muralidharan, C. Malcontenti-Wilson, W. McLaren, C. Christophi, Impact of blood flow occlusion on liver necrosis following thermal ablation, ANZ J. Surg. 76 (2006) 84–91.
[38] T. Su, J. Liao, Z. Dai, L. Xu, S. Chen, Y. Wang, et al., Stress-induced phosphoprotein 1 mediates hepatocellular carcinoma metastasis after insufficient radiofrequency ablation, Oncogene 37 (2018) 3514–3527.
[39] B.A. Reynolds, S. Weiss, Generation of neurons and astrocytes from isolated cells of the adult mammalian central nervous system, Science 255 (1992) 1707–1710.
[40] C. Raggi, M. Correnti, A. Sica, J.B. Andersen, V. Cardinale, D. Alvaro, et al., Cholangiocarcinoma stem-like subset shapes tumor-initiating niche by educating associated macrophages, J. Hepatol. 66 (2017) 102–115.
[41] R.P. Verma, C. Hansch, Matrix metalloproteinases (MMPs): chemical–biological functions and (Q)SARs, Bioorg. Med. Chem. 15 (2007) 2223–2268.
[42] T. Oskarsson, E. Batlle, J. Massague, Metastatic stem cells: sources, niches, and vital pathways, Cell Stem Cell 14 (2014) 306–321.
[43] M. Ahmed, C.L. Brace, F.J. Lee, S.N. Goldberg, Principles of and advances in percutaneous ablation, Radiology 258 (2011) 351–369.
[44] M.J. Cudmore, P.W. Hewett, S. Ahmad, K. Wang, M. Cai, B. Al-Ani, et al., The role of heterodimerization between VEGFR-1 and VEGFR-2 in the regulation of endothelial cell homeostasis, Nat. Commun. 3 (2012).